Journal of Sound and Vibration (2000) **229**(3), 453–466
doi:10.1006/jsvi.1999.2506, available online at http://www.idealibrary.com on IDEAL®

MODELLING THE VIBRATION BEHAVIOUR OF INFINITE STRUCTURES BY FEM

C. WANG AND J. C. S. LAI

Acoustics and Vibration Unit, School of Aerospace and Mechanical Engineering, The University of New South Wales, Australian Defence Force Academy, ACT 2600, *Australia*

(*Received* 25 *March* 1999, *and in final form* 14 *June* 1999)

In vibration power flow analysis, often the vibration behaviour of infinite structures is required. The modelling of infinite structures using the finite element method has been discussed. By considering the impedance of a finite beam and finite plate, theoretical formulae for a spring–damper combination to match these impedances are derived. Examples are given for a rather short (200 mm) beam and a small (400 mm diameter) plate with spring–dampers applied to the edges of the structures using the finite element method. Results of the driving point mobility indicate that these finite structures simulate an infinite beam and an infinite plate very well. Furthermore, the surface mobility of an infinite plate over a square contact area subject to a uniform conphase force excitation has been calculated successfully using just under 8 times fewer elements than a previous study.

1. INTRODUCTION

In recent years, the vibration power flow in structures has received more and more attention because it provides fundamental understanding to the transmission of vibration and hence structure-borne sound, thus allowing effective control to be implemented. The vibration behaviour of infinite structures is essential for vibration power flow analysis as it has been demonstrated by Cremer *et al.* [1] that the power supplied to a finite system by a random force is equal to the power supplied by that force to a corresponding infinite system. Thus, considerable insight may be gained by studying the power flow in infinite structures. However, infinite structures do not exist in practice and it is not a trivial exercise to verify the theoretical results derived for infinite structures. Experimentally, one may use a finite structure with the edges embedded into sand which absorbs the incident energy but the results are usually acceptable only at high frequencies. Furthermore, one may wish to study the coupling between a finite structure and an infinite structure. An alternative approach to the experimental method is to use numerical methods, predominantly, the finite element method (FEM). For example, in their study of the dynamic interactions between the railway vehicle and track, Dong *et al.* [2] developed a finite element model of an infinitely long track. The objective of this paper is, therefore, to discuss the modelling of infinite structures by the finite

0022-460X/00/030453 + 14 $35.00/0

element method. In particular, both infinite beams and infinite plates will be considered and the results will be compared with the theoretical results.

2. THEORETICAL ANALYSIS

In the finite element method (FEM), an "infinite" structure has to be modelled using a finite structure because a truly "infinite" structure would require an infinite number of elements. The main difference between finite and infinite structures is that while wave reflections would occur at boundaries for finite structures, they would be absent for infinite structures. Therefore, if the wave reflection at the boundaries for finite structures could be eliminated, the vibration behaviour would basically be like that of the corresponding infinite structure.

According to the wave theory, wave reflection occurs where the wave impedance is not continuous (i.e., not matched). The wave impedance, in acoustics, is defined [3] as

$$Z_w = \frac{p}{u}, \tag{1}$$

where p is the sound pressure at a point in the medium, and u is the particle velocity at the same point. This parameter gives an indication of the acoustic energy transmission in the medium. Normally, it is a complex number which depends on the properties of the medium and the behaviour of the sound source, and could vary with the position in the medium. For an acoustic wave, if Z_w at a point in the medium is a real number and is equal to the specific acoustic impedance of the medium (ρc), the acoustic energy would propagate through this point without any loss and reflection. However, if Z_w is different from ρc, wave reflection would occur. Obviously, this mismatch of the wave impedance usually happens at the physical boundary of the medium, where there is a discontinuity in the specific impedance at the interface of two media. Therefore, in order to simulate an unbounded medium with a bounded medium, the wave impedance at the boundaries has to be adjusted so that the reflection wave can be totally eliminated without affecting the incident wave.

The waves in a structure are much more complicated than acoustic waves. Normally, there are three types of structural waves: longitudinal waves, transverse waves, and bending waves [1]. For longitudinal and transverse waves, since their equations of motion take the same form as those of acoustic waves which are longitudinal waves, the discussion made above should apply. However, for bending waves, since the equation of motion is a fourth order partial differential equation, the characteristics of bending waves would be different from those of longitudinal and transverse waves. Since the bending motion of a structure is a major concern in vibro-acoustic analysis, some basic concepts about bending waves are reviewed below.

Unlike other waves, bending waves must be represented by four field variables instead of two. Normally, the transverse velocity u, the angular velocity Ω, the

bending moment M, and the shear force F are four variables commonly used in the analysis. Consider a one-dimensional bending wave propagating in the x direction as an example. The spatial relationships between these variables and the transverse displacement η can be written as [1] (omitting the time component $e^{j\omega t}$, without loss of generality)

$$u(x) = j\omega\eta(x), \qquad \Omega(x) = j\omega\frac{d\eta(x)}{dx}, \qquad M(x) = -B\frac{d^2\eta(x)}{dx^2}, \qquad F(x) = B\frac{d^3\eta(x)}{dx^3}, \tag{2}$$

where j is the imaginary number $\sqrt{-1}$, t is time, ω is the angular frequency and B is the bending stiffness. Since at a given point, the motion of a structural element includes the movement due to the variation of the shear force $F(x)$, as well as the rotation due to the variation of the bending moment $M(x)$, the power transmitted through this point consists of the power due to the bending moment P_M and that due to the shear force P_F, which can be expressed as [1]

$$P_M(x) = \tfrac{1}{2}\,\mathrm{Re}[M(x)\cdot\Omega(x)^*],$$
$$P_F(x) = \tfrac{1}{2}\,\mathrm{Re}[F(x)\cdot u(x)^*]. \tag{3}$$

Here the superscript $*$ represents complex conjugate. For a plane wave of the form $\eta(x) = Ae^{-jkx}$, where A is the amplitude and k is the wavenumber, it has been shown that P_M and P_F are out of phase by a quarter period [1]. This means that when P_M is maximum, P_F is zero. Also, the force wave impedance Z_f and the moment wave impedance W_m for a plane wave can be shown as [1]

$$Z_f(\omega) = \frac{F(x)}{u(x)} = \frac{Bk^3}{\omega}, \qquad W_m(\omega) = \frac{M(x)}{\Omega(x)} = \frac{Bk}{\omega}. \tag{4}$$

In order to examine the wave reflection at the boundary, two typical structures, namely, a beam and a plate, are analyzed below.

2.1. BEAM

Assume a semi-infinitely long beam in which a bending wave is approaching the end. Owing to the discontinuity of the beam at the boundary, a reflection wave would be generated. Also, a decay term would happen near the boundary. The general solution of the vibration displacement can be written as [4]

$$\eta(x) = A_1e^{-jkx} + A_2e^{jkx} + A_3e^{kx}, \tag{5}$$

where A_1, A_2, and A_3 are three constants dependent on the boundary conditions of the beam. Three typical boundary conditions are: simply supported, clamped and free, which can be expressed by [4]

$$\eta(x)|_{x=x_0} = 0, \qquad \left.\frac{\mathrm{d}^2\eta(x)}{\mathrm{d}x^2}\right|_{x=x_0} = 0 \quad \text{for a simply supported end,}$$

$$\eta(x)|_{x=x_0} = 0, \qquad \left.\frac{\mathrm{d}\eta(x)}{\mathrm{d}x}\right|_{x=x_0} = 0 \quad \text{for a clamped end,}$$

and

$$\left.\frac{\mathrm{d}^3\eta(x)}{\mathrm{d}x^3}\right|_{x=x_0} = 0, \qquad \left.\frac{\mathrm{d}^2\eta(x)}{\mathrm{d}x^2}\right|_{x=x_0} = 0 \quad \text{for a free end.}$$

It can be seen that for a clamped end, the force impedance and the moment impedance are both infinite due to the zero lateral displacement and the zero angular displacement. For a simply supported boundary, the force impedance is infinite, while the moment impedance is zero because of the zero moment. For a free end, the force impedance and the moment impedance are both zero. Obviously, since the impedance at the boundary is different from the characteristic impedance of the structural material, wave reflection would occur at the boundary.

To change the impedance at the boundary, a simple way is to introduce a spring–damper element, as shown in Figure 1. The impedance of a spring–damper can be written as

$$Z(\omega) = C + \frac{K}{\mathrm{j}\omega}, \tag{6}$$

where C is the damping coefficient, and K is the spring stiffness. Since for the simply supported and clamped end, the lateral displacement is forced to zero, the spring–damper is only applicable to the free end.

At the free end connected to a spring–damper, the shear force $B(\mathrm{d}^3\eta(x)/\mathrm{d}x^3)$ is no longer zero due to the coupling. However, since the spring–damper shown in Figure 1 does not affect the moment at this point, the moment is still zero at the end. Thus,

$$M(x)|_{x=0} = -B\left.\frac{\mathrm{d}^2\eta(x)}{\mathrm{d}x^2}\right|_{x=0} = B(k^2A_1\mathrm{e}^{-\mathrm{j}kx} + k^2A_2\mathrm{e}^{\mathrm{j}kx} - k^2A_3\mathrm{e}^{kx})|_{x=0} = 0 \tag{7}$$

which gives

$$A_3 = A_1 + A_2. \tag{8}$$

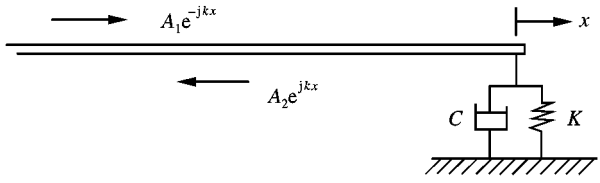

Figure 1. A semi-infinite beam with a spring–damper system at one end.

The shear force at the free end should be equal to the force of the spring–damper, which can be written as

$$B\frac{\mathrm{d}^3\eta(x)}{\mathrm{d}x^3}\bigg|_{x=0} = \mathrm{j}\omega Z(\omega)\eta(x)|_{x=0}. \tag{9}$$

Substituting equations (5) and (6) into equation (9), we have

$$\left(\frac{Bk^3}{\omega} - C + \mathrm{j}\frac{K}{\omega}\right)A_1 + \left(-\frac{Bk^3}{\omega} - C + \mathrm{j}\frac{K}{\omega}\right)A_2 + \left(-\mathrm{j}\frac{Bk^3}{\omega} - C + \mathrm{j}\frac{K}{\omega}\right)A_3 = 0. \tag{10}$$

By using equation (8), equation (10) becomes

$$\left[\frac{Bk^3}{\omega}(1-\mathrm{j}) - 2C + \mathrm{j}\frac{2K}{\omega}\right]A_1 + \left[-\frac{Bk^3}{\omega}(1+\mathrm{j}) - 2C + \mathrm{j}\frac{2K}{\omega}\right]A_2 = 0. \tag{11}$$

Since A_1 is the amplitude of the incident wave which must not be zero, for equation (11) to be always valid, we must have

$$\frac{Bk^3}{\omega}(1-\mathrm{j}) - 2C + \mathrm{j}\frac{2K}{\omega} = 0,$$
$$A_2 = 0. \tag{12}$$

Equation (12) therefore indicates that if the damping coefficient C, and the spring stiffness K satisfy the relationships

$$C = \frac{Bk^3}{2\omega}, \qquad K = \frac{Bk^3}{2} \tag{13}$$

the reflection wave can be suppressed. In order to examine the power transmission in the beam under this circumstance, substituting equation (13) back to equations

(2) and (5), we have

$$\eta(x) = A_1(\mathrm{e}^{-\mathrm{j}kx} + \mathrm{e}^{kx}), \quad M(x) = Bk^2A_1(\mathrm{e}^{-\mathrm{j}kx} - \mathrm{e}^{kx}), \quad F(x) = Bk^3A_1(\,\mathrm{j}\mathrm{e}^{-\mathrm{j}kx} + \mathrm{e}^{kx}). \tag{14}$$

It can be seen that although the reflection wave has been eliminated, an exponentially decaying near field still exists. However, in the far field (i.e., large negative x) where the term e^{kx} can be neglected, it can be easily proved that the wave impedance is the characteristic impedance. In the near field, the force wave impedance can be obtained from equation (13):

$$Z_f(x, \omega) = \frac{Bk^3}{\mathrm{j}\omega}\frac{\mathrm{j}\mathrm{e}^{-\mathrm{j}kx} + \mathrm{e}^{kx}}{\mathrm{e}^{-\mathrm{j}kx} + \mathrm{e}^{kx}}. \tag{15}$$

Obviously, this impedance is a complex number which means there is energy storage in the near field. At $x = 0$, $Z_f = Bk^3(1 - \mathrm{j})/2\omega$. Note that the impedance of the spring–damper is also $Z = Bk^3(1 - \mathrm{j})/2\omega$. Therefore, the energy stored in the near field would be exchanged with that in the spring–damper without affecting the power transmission of the active power. To verify this, the power due to the shear force and the moment can be obtained by using equations (3) and (14):

$$\begin{aligned} P_F(x) &= \tfrac{1}{2}\mathrm{Re}[F(x)\cdot u(x)^*] = \tfrac{1}{2}B\omega k^3|A_1|^2[1 + (\cos kx + \sin kx)\mathrm{e}^{kx}], \\ P_M(x) &= \tfrac{1}{2}\mathrm{Re}[M(x)\cdot \Omega(x)^*] = \tfrac{1}{2}B\omega k^3|A_1|^2[1 - (\cos kx + \sin kx)\mathrm{e}^{kx}]. \end{aligned} \tag{16}$$

It can be seen that at any position of the beam, including the near field, the total power transmitted is always a constant ($= B\omega k^3|A_1|^2$). Also, at $x = 0$, the power due to the moment is zero, while the total power is carried by the shear force and the corresponding lateral movement. This therefore guarantees that by only applying one spring–damper at the free end of the beam, the reflection wave can be efficiently suppressed.

2.2. PLATE

The bending wave in a plate is two-dimensional. In order to facilitate the analysis, a circular plate is chosen, as shown in Figure 2. For a circular plate, the general solution of the vibration displacement can be written by employing the polar co-ordinates as [1]

$$\eta(r, \theta) = [A'_1H_n^{(2)}(-\mathrm{j}kr) + A'_2H_n^{(2)}(kr) + A'_3H_n^{(1)}(kr) + A'_4H_n^{(1)}(-\mathrm{j}kr)]\cos(n\theta + \varphi), \tag{17}$$

where $H_n^{(1)}(\cdot)$, $H_n^{(2)}(\cdot)$ are Hankel functions of the first and second kind, respectively, A'_1, A'_2, A'_3, A'_4 and ϕ are five constants dependent on the boundary conditions

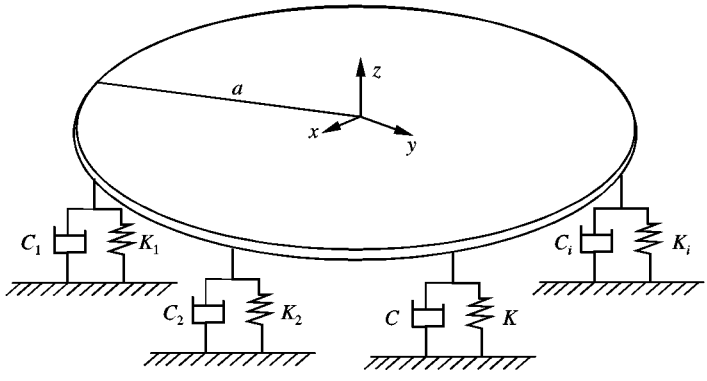

Figure 2. A circular plate with spring–dampers distributed along the boundary.

of the plate, and n is an integer denoting the mode order of the circumferential modes.

Since the vibration solution near the boundary of a plate is of interest, by assuming the boundary is in the far field of the excitation region, equation (17) can be simplified by using the large value expressions of the Hankel functions:

$$\eta(r, \theta) = \left[A_1 \frac{e^{-jkr}}{\sqrt{r}} + A_2 \frac{e^{jkr}}{\sqrt{r}} + A_3 \frac{e^{kr}}{\sqrt{r}} \right] \cos(n\theta + \varphi) \tag{18}$$

Here A_1, A_2 and A_3 are constants, and the term $e^{-kr}/\sqrt{r}$ corresponding to $H_n^{(2)}(-jkr)$ in equation (17) is neglected in equation (18) because of the farfield assumption. From equation (18) it can be clearly seen that to make this circular plate behave like an infinite plate, the amplitude of the reflection wave (A_2) has to be zero by changing the impedance at the boundary.

In section 2.1, it was shown that the force impedance can be applied only to the free end of the structure. Therefore, when introducing the force impedance $Z(\omega)$ at the free edge of the plate, the boundary conditions can be written as [4]

$$M(r, \theta)|_{r=a} = -B \left[\frac{\partial^2 \eta(r, \theta)}{\partial r^2} + \frac{\mu}{r} \frac{\partial^2 \eta(r, \theta)}{\partial \theta^2} + \frac{\mu}{r} \frac{\partial \eta(r, \theta)}{\partial r} \right]_{r=a} = 0,$$

$$F(r, \theta)|_{r=a} = B \left[\frac{\partial^3 \eta(r, \theta)}{\partial r^3} + \frac{2-\mu}{r} \frac{\partial^2 \eta(r, \theta)}{\partial r^2} - \frac{2-\mu}{r^2} \frac{\partial \eta(r, \theta)}{\partial r} + \frac{2-\mu}{r^2} \frac{\partial^2 \eta(r, \theta)}{\partial \theta^2 \partial r} + \frac{2(2-\mu)}{r^3} \frac{\partial^2 \eta(r, \theta)}{\partial \theta^2} \right]_{r=a}$$

$$= j\omega Z(\omega) \eta(r, \theta)|_{r=a}. \tag{19}$$

By substituting equation (18) into equation (19), and by neglecting the small terms for large ka (farfield assumption), we have

$$A_3 e^{ka} = A_1 e^{-jka} + A_2 e^{jka}, \tag{20a}$$

$$A_1 e^{-jka}\left[jk^3 - \frac{j\omega Z(\omega)}{B}\right] + A_2 e^{jka}\left[-jk^3 - \frac{j\omega Z(\omega)}{B}\right] + A_3 e^{ka}\left[k^3 - \frac{j\omega Z(\omega)}{B}\right] = 0. \tag{20b}$$

By substituting equation (20a) into equation (20b), for $A_2 = 0$ one can obtain

$$Z(\omega) = \frac{Bk^3(1-j)}{2\omega}. \tag{21}$$

This result indicates that by introducing a force impedance properly, the wave reflection at the boundary of a circular plate can be effectively eliminated. However, it should be noted that equation (21) is obtained by invoking the farfield assumption. Therefore, strictly speaking, the amplitude of the reflection wave (A_2) would only be very small rather than exactly zero by making the force impedance satisfy equation (21) at the boundary of a circular plate. Actually, for a more general and rigorous analysis, it can be found that to make A_2 exactly zero, the force impedance at the boundary may depend on the angle of the incident wave to the boundary. This makes the modelling of an infinite plate more difficult and complicated. However, equation (21) may be a good enough approximation.

Like modelling infinite beams, a force impedance may be introduced at the boundary of a circular plate by using a series of spring–dampers, as shown in Figure 2. Note that equation (21) is the force impedance per unit length. By combining equation (6) with equation (21), the damping coefficient C, and the spring stiffness K for each spring–damper is

$$C_i = \frac{Bk^3}{2\omega}\Delta l_i, \qquad K_i = \frac{Bk^3}{2}\Delta l_i, \tag{22}$$

where Δl_i is the equivalent length that the ith spring–damper takes effect. If the spring–dampers are distributed uniformly, $\Delta l_i = 2\pi a/N$, where N is the total number of the spring–dampers used.

3. FEM MODELLING

In order to verify the above results and model the vibration behaviour of infinite beams and plates by the finite element method, a commercial FEM code, ANSYS 5.4, was used. All the calculations were made on a SUN ENTERPRISE 4500 workstation.

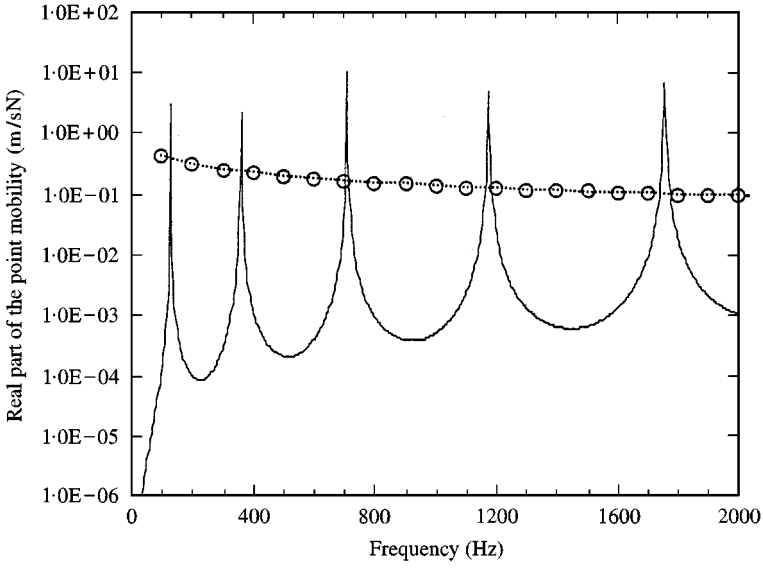

Figure 3. The real part of the driving point mobility spectrum of a beam. —— finite length 0·2 m; ..... infinite model (0·2 m); ○ theory [1].

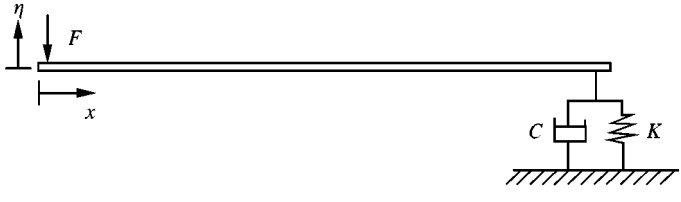

Figure 4. A finite beam with a spring–damper at one end.

3.1. INFINITE BEAM

A steel beam with length 200 mm, 1 mm in thickness and 10 mm in width was firstly created using 20 BEAM3 elements and 21 nodes. By setting the two ends free and applying a point force at one end of the beam, the real part of the driving point mobility can be obtained by using the Harmonic Analysis in ANSYS. The results are shown in Figure 3. It can be seen that there are distinct peaks due to the vibration modes of the beam. In order to simulate an infinite beam, a spring–damper was then applied to the other end of the beam, as shown in Figure 4. In ANSYS, a spring–damper was modelled as an element with two nodes, one coupled to the beam and the other fixed. The element type was COMBIN14. Since the damping coefficient and the stiffness of the spring–damper change with frequency as shown in equation (13), substep files have to be created in ANSYS for each frequency so that the damping coefficient and the stiffness of the spring–damper can change accordingly. In the calculations, 20 substep files were created for 20 frequencies from 100 to 2000 Hz with a step of 100 Hz. Since for a semi-infinite

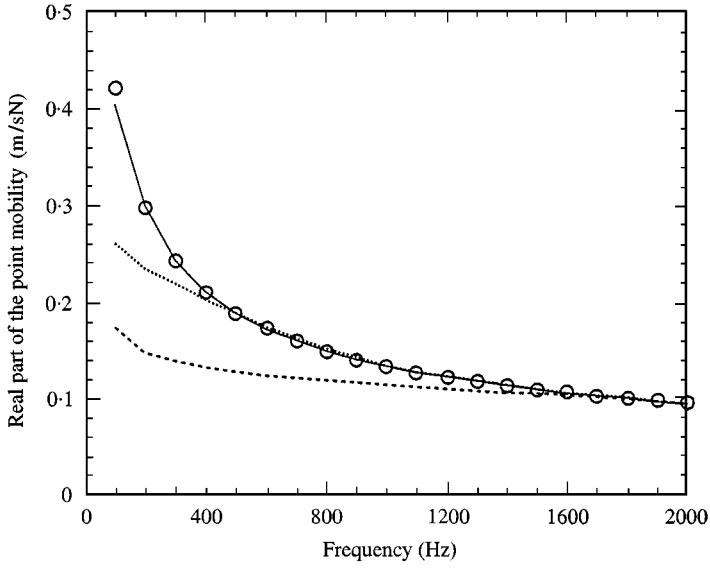

Figure 5. The real part of the driving point mobility spectrum of an infinite beam. —— $l = 0{\cdot}2$ m; ..... $l = 0{\cdot}1$ m; - - - - $l = 0{\cdot}05$ m; ○ theory [1].

beam excited at one end, there would be no vibration modes, the Full method was used for the Harmonic Analysis in ANSYS. The real part of the driving point mobility is shown in Figure 3. It can be seen that the curve is quite smooth, indicating that wave reflection at the other end is effectively eliminated by the spring–damper. These results agree very well with the theoretical results of Cremer *et al.* [1].

In order to evaluate the effects of the length of finite beams on the modelling results, two more beams 100 and 50 mm in length, respectively, were used. The number of elements per unit length was kept the same at 1 per 10 mm. The real part of the driving point mobility for these three beams is shown in Figure 5. It can be seen that as the finite beam becomes shorter, the discrepancies at low frequencies become more significant. This is because at low frequencies, the near-field region becomes larger and may include the excitation point, thus changing the response at the driving point. On the other hand, the excitation would also have its own near field which is neglected in our analysis. When this near field extends to the end with the spring–damper attached, obviously the incident power may not be fully absorbed by the spring–damper designed without considering the effects of the near field. Therefore, in order to model the vibration behaviour of an infinite beam by introducing a force impedance, the finite length beam should be chosen to be at least 200 mm for a low-frequency limit of 100 Hz, based on the results in Figure 5.

3.2. INFINITE PLATE

In order to model the vibration behaviour of an infinite plate, a steel circular plate 200 mm in radius, and 1 mm in thickness was created using 640 SHELL63

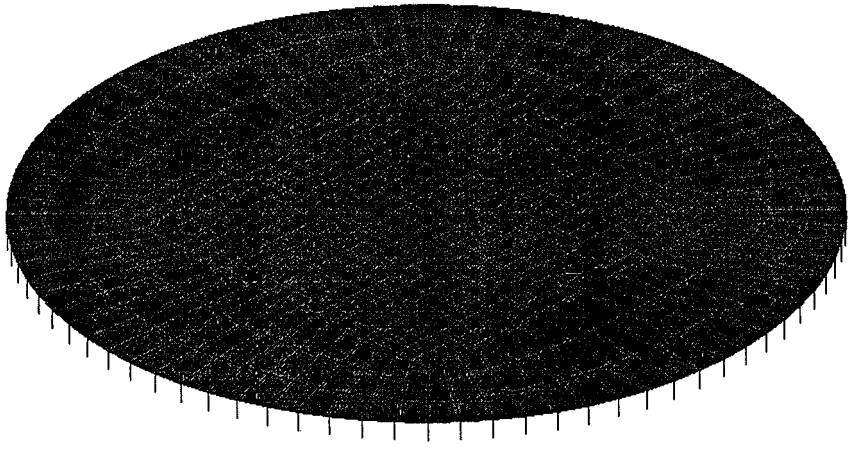

Figure 6. Finite element model of a circular plate.

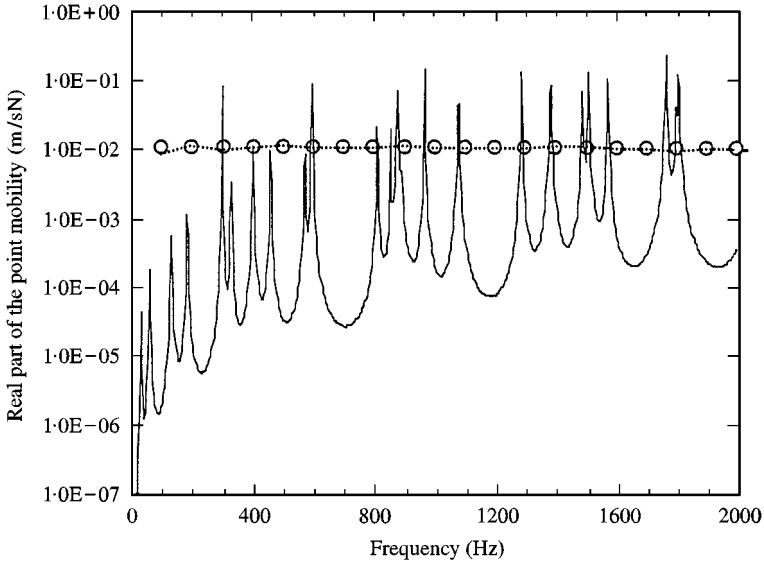

Figure 7. The real part of the driving point mobility spectrum of a plate. —— finite plate; ..... infinite plate model; ○ theory [1].

elements and 681 nodes, as shown in Figure 6. Note that the finite element model consists of a square region to simulate the surface mobility of a square contract area, as discussed in section 3.3 below. When the plate is excited by a point force at $r = 105$ mm, the real part of the driving point mobility calculated by ANSYS is shown in Figure 7. It can be seen that corresponding to each vibration mode of this circular plate, there is a peak in the driving point mobility. To simulate an infinite plate using this circular plate, 80 spring–dampers were attached to the 80 nodes at the edge of the plate, as shown in Figure 6. Also 20 substep files were used for frequencies from 100 to 2000 Hz with a step of 100 Hz. When a point force is

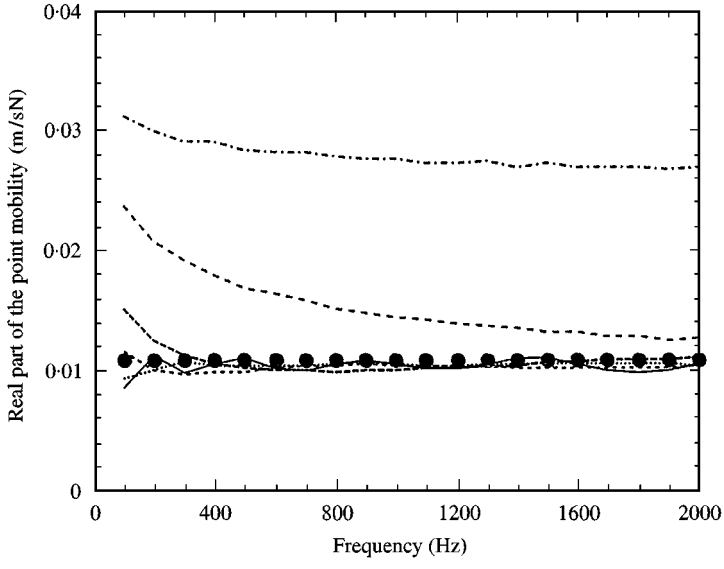

Figure 8. The real part of the driving point mobility spectrum of an infinite plate model. —— $r = 0$; - - - - $r = 0{\cdot}12$ m; – – – $r = 0{\cdot}183$ m; ····· $r = 0{\cdot}06$ m; – – – $r = 0{\cdot}15$ m; – · – · – $r = 0{\cdot}2$ m; ● theory [1].

applied at the centre of the plate, by using the Full method for the Harmonic Analysis in ANSYS, the driving point mobility can be obtained. It can be seen from Figure 7 that the FEM results of the driving point mobility agree very well with the theoretical result for an infinite plate given by Cremer *et al.* [1]

In order to further examine the infinite extent of this plate model, the driving point mobility at different distances r from the centre of the plate was calculated, as shown in Figure 8. It can be seen that as the excitation position approaches the edge of the plate, the discrepancies between the theoretical results and the FEM results become larger, especially at low frequencies. This is due to the influence of the decay field near the plate boundary and the excitation position. In particular, when the force was applied at the edge, the real part of the driving point mobility is not of the nature of an infinite plate. Therefore, for the plate model used here, there is a region, for example $r < 150$ mm, in which the plate vibrates like an infinite plate. However, it can be seen from Figure 8 that even within this region, the agreement between the FEM and the theoretical results are not perfect even at high frequencies. This is because, as stated in section 2.2, equation (21) is obtained by invoking some simplifications. Nevertheless, the accuracy shown in Figure 8 appears to be good enough for vibro-acoustic analysis using a 400 mm diameter circular plate for frequencies above 300 Hz.

3.3. SURFACE MOBILITY OVER A SQUARE CONTACT AREA OF AN INFINITE PLATE

In the study of vibration isolation, the mobility of a source or receiving structure is often employed in the analysis of the dynamic characteristics of build-up systems.

Classical mobility methods simplify the excitation area between two subsystems as a point-like contact, hence the necessity of calculating the point mobility. However, in a practical situation, almost every contact area between a machine and its supporting structure has a characteristic dimension which is not negligible. For flexural waves in a plate, if the dimensions of the contact area are larger than approximately 10 percent of the governing wavelength [1], point mobility estimates can lead to significant errors. Thus the mobility over a finite contact area, known as surface mobility, has to be considered. The surface mobility of an infinite thin plate over a square contact area subject to a uniform conphase force excitation has been formulated theoretically by Dai *et al.* [5] using the effective point mobility concept and complex power approach. The theoretical result has been verified numerically and experimentally by Dai *et al.* [6]. In the numerical calculations of the surface mobility, Dai *et al.* [6] employed the finite method to simulate an infinite plate by using a very large plage (4·8 m × 9·6 m) and curve-fitting techniques to smooth out the peaks in the mobility due to imperfect simulation. In the FEM calculations made by Dai *et al.* [6], they used 4896 elements. It is, therefore, interesting to compare these results with the results of the surface mobility obtained by a 400 mm diameter circular plate as shown in Figure 6. The circular plate model consists of 400 elements over a square area of 212 mm × 212 mm and 240 elements over the remaining area. There were 100 substep files for frequencies from 50 to 5000 Hz with a step of 50 Hz. The surface mobility is calculated using the effective point mobility by discretizing the square contact area into 3×3 points and 9×9 points, respectively, and the results are plotted in Figure 9 as a function of Helmholtz number $kw/2$ based on the halfwidth of the contact area. Note that in

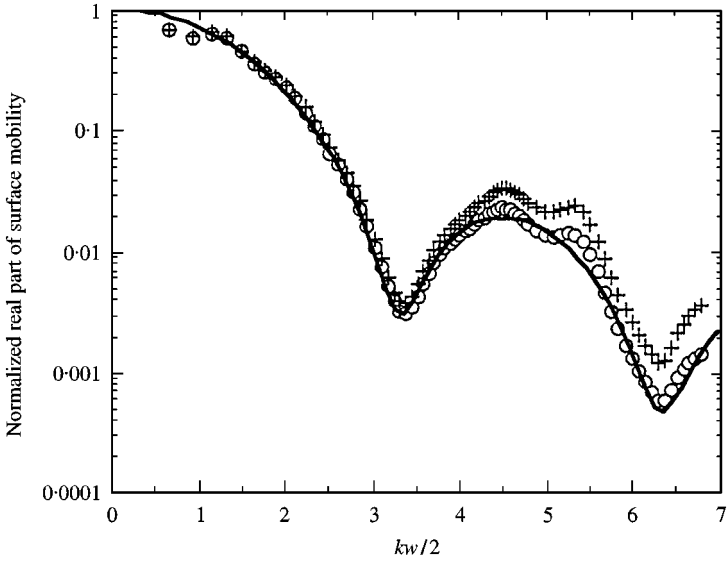

Figure 9. The surface mobility of an infinite plate over a square contact area subject to a uniform conphase force distribution. —— theoretical; + 9 points (FEM); ○ 81 points (FEM).

Figure 9, the surface mobility has been normalized using the point mobility. The discrepancies between the calculations for 9 and 81 points are mainly a result of discretization error. There is generally a very good agreement between the results of the 81 points and those of the theoretical method. The small differences at Helmholtz numbers less than 1 are due to the effect of the near field which has been neglected in the modelling. The small differences between the FEM and theoretical results that emerge at Helmholtz numbers greater than 5 are due to a mesh that may not be fine enough. At a Helmholtz number of 6, the number of elements per wavelength is only 3·5 based on the largest element and 10 based on the smallest element.

4. CONCLUSIONS

Theoretical analysis of the impedance of a finite structure such as a beam and a plate has been conducted. These results allow an infinite beam and an infinite plate to be simulated by the finite element method using a finite structure with appropriate spring–dampers applied to the boundaries of the structure. Examples given here show that a beam as short as 200 mm with only 20 elements yields results in good agreement with classical theoretical values for frequencies greater than 100 Hz. Furthermore, by using a 400 mm diameter plate with 640 elements, both the driving point mobility and the surface mobility over a square contact area are in good agreement with results obtained by the theoretical method for an infinite plate. These examples demonstrate the feasibility of using finite structures with spring–dampers to simulate infinite structures by the finite element method.

ACKNOWLEDGMENT

This project has been partially supported by the University College Rector Special Research Grant.

REFERENCES

1. L. Cremer, M. Heckl and E. Ungar 1988 *Structure-Borne Sound*. Berlin: Springer, second edition.
2. R. G. Dong, S. Sankar and R. V. Dukkipati 1994 *Proceedings of the Institution of Mechanical Engineers Part F: Journal of Rail and Prapid Transit* **208**, 61–72. A finite element model of railway track and its application to the wheel flat problem.
3. L. E. Kinsler, A. R. Frey, A. B. Coppens and J. V. Sanders 1982 *Fundamentals of Acoustics*. New York: Wiley, third edition.
4. W. Soedel 1993 *Vibration of Shells and Plates*. New York: Marcel Dekker, second edition.
5. J. Dai, J. C. S. Lai, H. M. Williamson and Y. J. Li 1999 *Journal of Sound and Vibration* **225**, 831–844. Investigation of vibration power transmission over a rectangular excitation area using effective point mobility.
6. J. Dai, J. C. S. Lai, Y. J. Li and H. M. Williamson 1999 *Applied Acoustics*. Surface mobility over a square contact area of an infinite plate: experimental measurements and numerical prediction (accepted).